doi:10.26443/seismica.v5i2.1779

SEISMICA

Revisiting the causal factors of seismicity in the Dallas–Fort Worth area

Iason Grigoratos *[1], **Alexandros Savvaidis** [2], **Heather R. DeShon** [3], **Stefan Wiemer** [4]

[1]Swiss Seismological Service, ETH Zurich, Switzerland (previously), [2]Bureau of Economic Geology, University of Texas at Austin, USA, [3]Dept. of Earth Sciences, Southern Methodist University, USA, [4]Swiss Seismological Service, ETH Zurich, Switzerland

Author contributions: *Conceptualization*: I.G., A.S.. *Data Curation*: I.G., A.S., H.D.. *Formal Analysis*: I.G. *Funding Acquisition*: I.G., A.S., S.W.. *Investigation*: I.G., A.S., H.D.. *Methodology*: I.G., A.S.. *Project Administration*: A.S., S.W.. *Resources*: A.S., S.W.. *Software*: I.G.. *Supervision*: A.S.. *Validation*: I.G., A.S., H.D.. *Visualization*: I.G.. *Writing – original draft*: I.G., A.S.. *Writing – review & editing*: I.G., A.S., H.D..

Abstract The seismicity levels in the Fort Worth basin over the last 15 years have been elevated, with one earthquake above magnitude 4 occurring in 2015. Wastewater disposal (SWD) for oil and gas activities has been reported as the causal factor. We applied an established probabilistic framework to examine the extent to which either SWD or hydraulic fracturing (HF) are potential causal factors. Our framework employed new regional earthquake catalogs and established physics-based principles. We first hindcasted the seismicity rates after 2008 on a spatial grid using either HF or wastewater data as input, and then compared them against the null hypothesis of solely tectonic loading. We identified one unnamed sequence as induced by HF. A causal link between SWD and the Irving-Dallas and Lake Lewisville sequences is apparent for large diffusivity values. Curiously, our framework finds no significant link with SWD for the Venus, Azle or Cleburne earthquake clusters. That said, the method assumes a temporally consistent seismic response within each grid-cell, which does not appear to be the case in the basin. Rather, the basin is dominated by isolated sequences on a small percentage of faults. We conclude that the Fort Worth basin is not prone to widespread fault reactivation, allowing for effective mitigation measures.

Production Editor:
Andrea Llenos
Handling Editor:
Pathikrit Bhattacharya
Copy & Layout Editor:
Sarah Jaye Oliva

Received:
June 12, 2025
Accepted:
May 19, 2026
Published:
July 23, 2026

Non-technical summary The Dallas–Fort Worth region has experienced unusual earthquake activity since 2008, including a magnitude 4.0 earthquake near Venus in 2015. This study re-examines with updated data whether certain oil and gas operations initiated the triggering of earthquakes. The authors test two possible causes: hydraulic fracturing (HF) and wastewater disposal (SWD). They found that HF is only linked to one small seismic sequence near the Oklahoma border. A causal link between SWD and the Irving-Dallas and Lake Lewisville sequences is apparent only under certain assumptions about how pressure from injected fluids travels through rock. Curiously, the study did not find clear support for SWD being the trigger of the Venus, Azle–Reno, or Cleburne sequences. That said, the method assumes that the seismic response of each spatial block is consistent over time, which does not appear to be the case in the basin. The study concludes that the earthquake activity is isolated on a small percentage of faults, allowing for targeted small-scale mitigation measures.

1 Introduction

The Fort Worth basin (FWB) encompasses the Barnett Shale formation, which has served as a major shale-gas producing unit benefiting from hydraulic fracturing (HF) operations since 2004. Co-produced wastewater (SWD) during oil and gas production is disposed primarily into the underlying Ellenburger dolomitic limestone formation (Hornbach et al., 2016), which lies just above the crystalline Precambrian basement in most parts of the basin. The Barnett and Ellenburger formations and the underlying basement are linked by faults (Ewing et al., 1990; Magnani et al., 2017). The basin underlies much of the Dallas–Fort Worth (DFW) metropolitan area, with a population over 8 million.

In the past 15 years, there have been six main earthquake sequences in the basin (Figure 1). The 2008–2015 DFW Airport sequence, the 2009-2012 Cleburne earthquakes in southwest Johnson County (south of the DFW metroplex), the Azle–Reno sequence (northwest of Fort Worth), the Irving-Dallas sequence, the Lake Lewisville sequence and the 2015 M_w 4.0 Venus sequence in northeast Johnson County, which hosted the May 2015 M_w 4.0 earthquake, the largest ever recorded in the basin. Each of these sequences exhibits swarm-like behavior, rather than typical mainshock–aftershock characteristics (Quinones, 2021). Outside Johnson county, the sequences appear short-lived and spatially limited, contrary to the cascading seismic response often observed in parts of Oklahoma, West Texas, and Eagle Ford (Grigoratos et al., 2022, 2025a,b). Overall, the earthquake sequences in the FWB exhibit spatial correlation with SWD operations, with the bulk of seismicity occurring within 15 km of high-rate SWD wells (Quinones et al., 2019). In fact, from all the documented sequences only the Irving–Dallas and Lake Lewisville sequences have no SWD wells nearby. That said, the vast majority of

*Corresponding author: research@grigoratos.com, Now at XXX

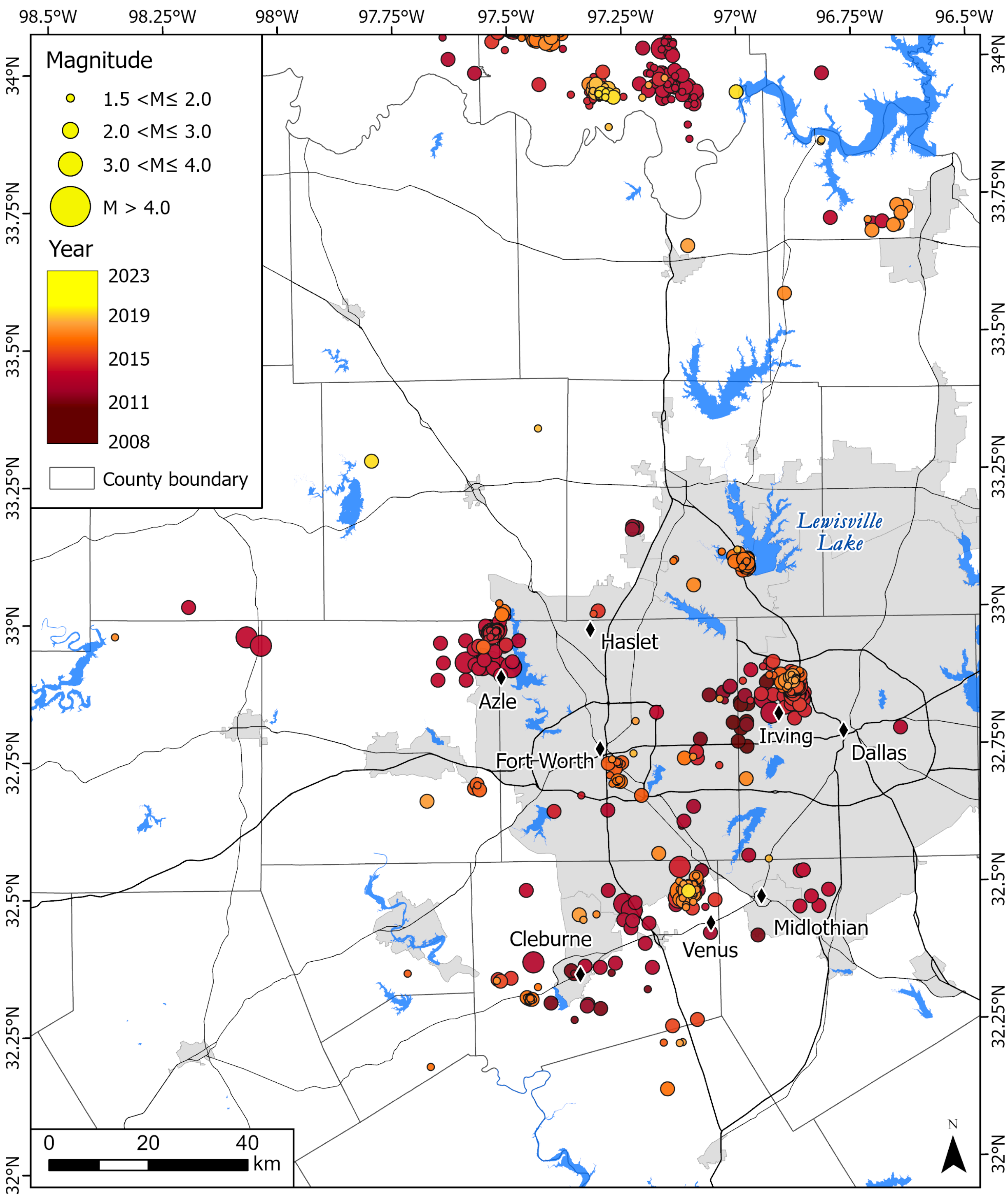

Figure 1 Map view showing the locations of all earthquakes above M 1.5 (circles) shaded by their time of occurrence and scaled by their magnitude. The county lines, urban areas (grey background), highways and lakes (light blue) are also shown. Black diamonds indicate key sites.

SWD wells have no detected earthquake nearby (Figure 2b). The same applies to HF wells.

Seismicity at the DFW Airport began in October 2008 with a series of earthquakes with magnitudes up to m_{bLg} 3.0, with a larger m_{bLg} 3.3 event occurring in May 2009. They were located just south of the airport at a depth of 4.8 km (Frohlich et al., 2010). Since January 2008, 13 wells had been drilled and hydraulically fractured in the Barnett Shale within 3 km of the cluster. These wells began production on dates ranging from June 2008 to March 2009 (Frohlich et al., 2011), so they could have been stimulated at any point between their drilling and production-start dates. Two SWD wells had also been drilled at that time, one northeast and one southwest of the DFW airport. The southwest SWD well is about 200 m south of the mean epicenter, much closer than any of the HF wells. The permitted disposal interval (3.3–4.2 km) is in the Ellenburger formation, only slightly above the initial focal depths of the earthquakes (Frohlich et al., 2010). Disposal at the southwest SWD well commenced on 12 September 2008, just seven weeks before the first DFW earthquakes were de-

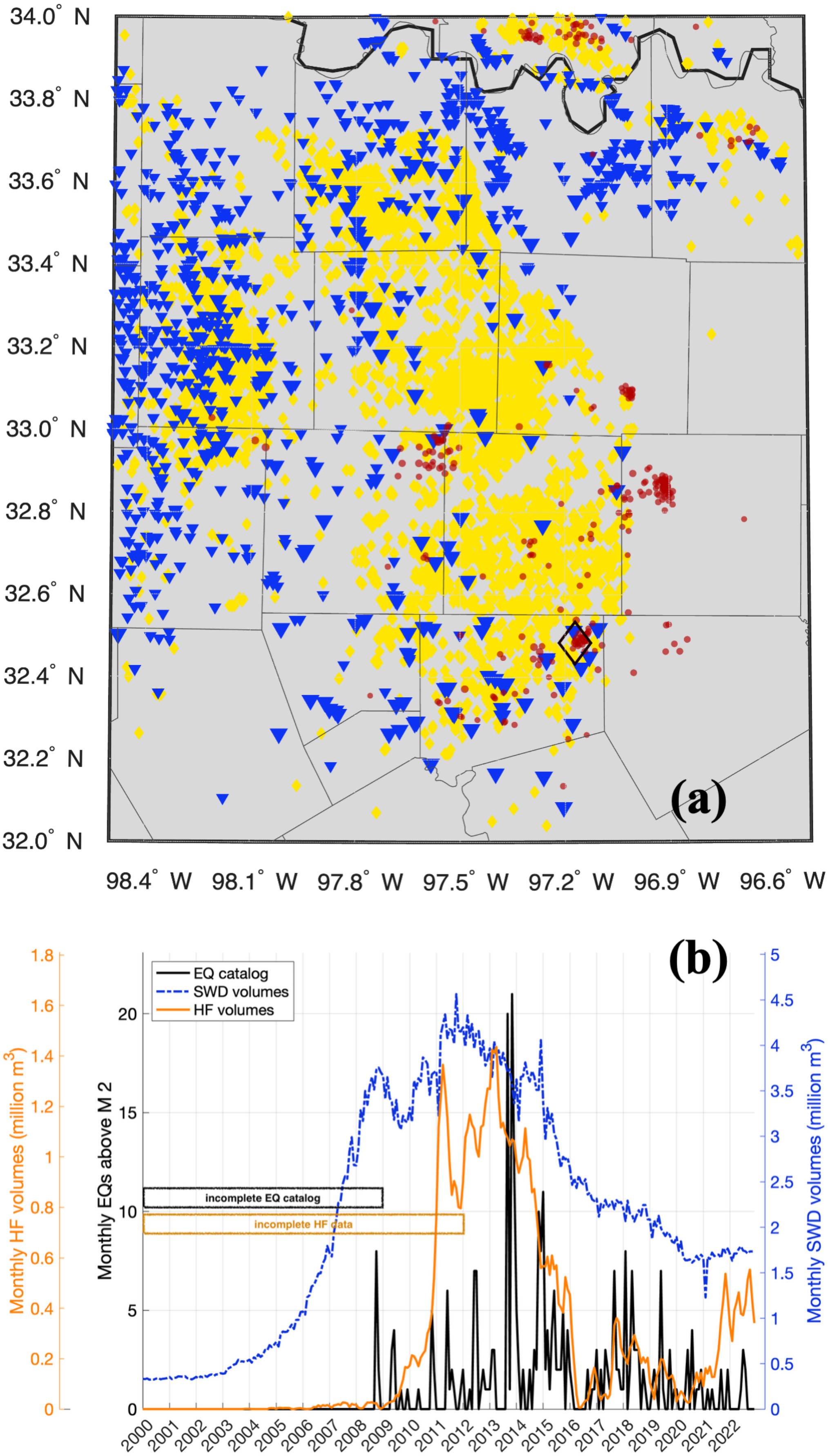

Figure 2 (a) Map of the investigated area showing declustered seismicity (M ≥ 2; red dots), wells (blue: SWD; yellow: HF) and county/state borders. The SWD wells are sized based on their total volume. The black diamond indicates the Venus earthquake in Johnson county (M_w 4.0). Data between 2000 and September 2022. (b) Time history of monthly HF and SWD volumes, and declustered seismicity rates for the investigated area shown in panel (a). The earthquake catalog is incomplete before 2009, while the HF data are incomplete before 2012.

tected. Both SWD wells reached disposal rates in excess of 250 thousand bbls/month (Frohlich et al., 2011). Ogwari et al. (2018) employed 3D pore-pressure diffusion modeling to suggest that the high-rate nearest SWD well is the primary driver of the seismicity. Since the shut-in of the nearest SWD well, the sequence continued into at least 2015 slowly migrating northeast along the 6 km causative fault (Ogwari et al., 2018).

On 9 June 2009, an m_{bLg} 2.8 earthquake near Cleburne was felt by a community that had never felt earthquakes in the past. The located events of this sequence were within 3 km from two SWD wells, less than a few hundred meters from the disposal depth, and not near other types of production activity (Justinic et al., 2013). One of these wells frequently had over 300 thousand bbls/month average rate since 2005. The felt earthquakes started a number of years after the initiation of the high-rate injector and between 6 and 8 months after the disposal rate was nearly doubled. Additionally, the earthquake activity decreased significantly six months after this injector was shut-in, while the closer injector continued to operate but with significantly smaller volumes of fluids (Justinic et al., 2013).

Beginning in November 2013, a series of earthquakes occurred near the city of Azle and Reno, about 25 km northwest of Fort Worth. As of 2015, the sequence includes eight earthquakes having magnitudes of 3 or greater; with the two largest and widely felt having m_{bLg} equal to 3.6 (Frohlich et al., 2016). The hypocentres were located within the Ellenburger formation and deeper within the basement (Quinones et al., 2019). Two high-volume wastewater injection wells and more than 70 production wells that produce gas and brine are situated within 10 km of the Azle earthquake sequence (Hornbach et al., 2015). Hornbach et al. (2015) concluded that on the basis of 3D pore-pressure modelling results and the absence of historical earthquakes near Azle/Reno, brine production combined with wastewater disposal represent the most likely cause of seismicity there. That said, coupled linear diffusion and poroelastic modeling by Zhai and Shirzaei (2018) found that the impacts of brine production on stress change and seismicity rate were negligible.

The Irving–Dallas sequence generated felt earthquakes, including two m_{bLg} 3.5 and 3.6 events on 6 January 2015 (DeShon et al., 2019). The events likely began as early as April 2014 (Quinones, 2021), and they were located within the basement (Quinones et al., 2019). This sequence remains the most enigmatic one in the basin; the causative fault is very far from both SWD and HF active wells (Figure 1; 2a). The sequence occurred on an optimally oriented fault for failure within the given stress field (Hennings et al., 2021), but it is unclear whether coupled pore pressure diffusion and/or poroelastic stress changes alone would be enough to induce slip on the fault (Quinones et al., 2019; Quinones, 2021). Both hydrogeologic (Gao et al., 2021) and geomechanical modelling (Quinones, 2021) support the possibility that cumulative injection in the basin triggered events in Irving-Dallas (e.g. Hornbach et al., 2016; Hennings et al., 2021). There is one set of inactive shale gas production wells (API 4211330147 & 4211330189) near the southern edge of the Irving-Dallas epicenters, further complicating interpretation. Based on public records through the Texas Railroad Commission, the sole producing well ceased production in 2012, and the two wells, drilled off the same pad, are the only known production wells in the region. The wells were by all accounts difficult to drill because the shale sits stratigraphically under the Ouachita Thrust, which moves hard metasediments over the production and injection units along the eastern margin of the basin. One well failed in 2009 due to a shallow casing failure during a hydrofracking stage and was shut in. The other well was low producing and has also been shut-in. It is possible that overpressure has developed in the problematic well and that these pressure changes have migrated down into the underlying units, but there is no data available to support or reject this speculation.

On 7 May 2015, a M_w 4.0 earthquake occurred in Johnson County, near Venus, not far from the Cleburne sequence. Five SWD wells were within 5 km of the Venus cluster and at a small vertical distance from its hypocenter. Most of the latter were located within the basement (Quinones et al., 2019). Scales et al. (2017) found that the events began nearly a decade prior to the M 4.0 earthquake and posited that the combined SWD led to an increase in subsurface pore fluid pressure that contributed to the triggering of this long-lived sequence, which continues to the present (2025). They also saw no definitive spatial or temporal correlation between individual SWD wells (in terms of start times, rates, or volumes) and the earthquake history.

Quinones et al. (2019) argued that in the geomechanical studies of Ogwari et al. (2018), Hornbach et al. (2016) and Zhai and Shirzaei (2018), stress changes associated with direct pore-pressure effects are highly concentrated at close distances to the wells, with poroelastic effects being a prerequisite for any far-field triggering of seismicity. Quinones et al. (2019) questioned, however, whether poroelastic stress changes alone were large enough to have induced slip far-field, given that the actual magnitude of the poroelastic stress changes is lower than the near-field pore-pressure effects (Segall and Lu, 2015). Notably, ever decreasing disposal rates from their peak levels in 2014 did not appear to coincide with consistently lower rates of seismicity across the basin through September 2022 (Figure 2b). In other words, the pre-2013 average seismicity rate is similar to the post-2013 rate.

Hennings et al. (2021) noted strong heterogeneity in the regional response of the FWB faults, with many non-seismogenic faults experiencing higher pore pressure increase compared to those that became seismogenic. Faults proximal to SWD operations became seismogenic at appreciably higher mean pore pressure increase than those in distal areas (their approach ignored poroelastic effects). Crucially, they found no straightforward relationship between pore pressure increases or FSP values, and the rate or maximum magnitude of earthquakes hosted on the same faults. FSP stands for fault slip potential and employs a linearized Mohr-Coulomb failure criterion, which defines critically stressed conditions by comparing the ratio of shear stress to effective normal stress on the fault before and after injection, and by considering the orientation and geometry of the fault relative to the regional stress field (Walsh and Zoback, 2016).

Figure 2a demonstrates that the link in space between SWD, HF and earthquake occurrence is not straightforward. In some cases, the seismicity is collocated with SWD or HF wells, but in most cases intense oil and gas activities have caused little to no detectable seismicity. Finally, despite the focus on SWD, the FWB hosts significant levels of HF activity that (at least) spatially overlaps with some of the aforementioned clusters (Figure 2a).

In this study, we apply for the first time an established probabilistic framework (Grigoratos et al., 2020a,b, 2022) to examine the extent to which both SWD and HF have contributed to elevated seismicity levels observed in FWB over the last 15 years. Our approach first hindcasts the seismicity rates after a given time on a spatial grid using either SWD or HF injection data as input, and then compares those rates against the null hypothesis of solely tectonic loading. In the end, each block is assigned a p-value, indicating the statistical confidence of its association with each oil and gas activity. Our analysis employed both declustered and non-declustered compilations of regional earthquake catalogs and established physics-based principles. This robust protocol has been previously successfully applied in Oklahoma (Grigoratos et al., 2020b, 2025b), West Texas (Grigoratos et al., 2022) and in the Eagle Ford shale play (Grigoratos et al., 2025a).

2 Data

First, we compiled a new unified earthquake catalog for the Central and Eastern United States (CEUS) with magnitudes above 1 over the time period of January 2000 to February 2023, merging multiple different sources (Table S1; Data and code availability section). TexNet (Savvaidis et al., 2019) and NTXES (Quinones et al., 2019) were the two main datasets for the FWB. Duplicate events among catalogs were removed following certain hierarchy rules, when more than one location or magnitude solution was available (Grigoratos et al., 2023). These rules, alongside the margins used during the duplicate-search are listed in Grigoratos and Wiemer (2023).

Local seismic research networks operated by Southern Methodist University (SMU) provided basic earthquake data for the FWB from October 2008 through January 2025. Notably this area was considered aseismic until 2008. TexNet added regional stations to the basin after 2017. The SMU network design aimed at resolving the depth and focal mechanism of small magnitude nearby earthquakes, and station deployments followed significant felt earthquakes and were of variable duration (DeShon et al., 2019). Local-distance recorded sequences in the dataset include the DFW Airport, Cleburne, Azle–Reno, Irving–Dallas, and Venus (Johnson county) sequences. These local studies have been unified into a single dataset, which has been termed the North Texas Earthquake Study Catalog (NTXES; Quinones et al., 2019; DeShon et al., 2019). The networks were not designed for regional earthquake monitoring within the FWB (Quinones et al., 2019), and thus there are significant spatio-temporal variations in the value of M_c and in epicentral uncertainty. Despite these limitations, the estimated regional M_c is reported to be around 2.1 after the year 2013, with the earthquakes rupturing normal faults located primarily within the Precambrian basement formation (Quinones et al., 2019). The EarthScope USArray data passed through the FWB with a 70-km station spacing between November 2009 and September 2011. Frohlich (2012) documented earthquakes down to magnitude 1.5 occurring across the basin in discrete clusters, nearly eight times the rate reported in ComCat over the same time period. When SMU, TexNet and USArray stations were not deployed within the basin, the backbone USGS stations reported earthquakes, though with higher estimated uncertainties. Thus, we opted for a magnitude of completeness (M_c) value of 2 for our investigation period. The latter started in October 2008 based on the completeness of the earthquake catalog and ended in September 2022 for HF and in December 2021 for SWD, in line with the completeness of the injection datasets. The methods we used in this study are not sensitive to the M_c (Grigoratos et al., 2022) and thus including more events by slightly underestimating the M_c is not an issue.

Our sourcing and processing of the HF and wastewater disposal data (Data and code availability section) followed the work by Grigoratos et al. (2022) and is described in Appendix A (Supplementary Material). Due to reporting lags, at the time of the analysis, the regional HF and SWD data were considered complete through September 2022 and December 2021, respectively. The gridded spatial distribution of cumulative HF stimulation days and SWD volumes are mapped in Figures S1 and S2a, respectively. The median depth of a HF and SWD well is around 2200 m and 1100 m, respectively. We used all SWD wells in our analysis, and not just the ones targeting the Ellenburger formation. The median duration of a HF stimulation was 4 days, and the median daily volume of a HF well was 10800 bbls.

3 Methods

3.1 Declustering

The earthquake recurrence models we use in this study can only model mainshocks (Grigoratos et al., 2020a). Grigoratos and Wiemer (2023) removed foreshocks and aftershocks from their CEUS catalog, assuming an M_c of 2 after 2008, using the declustering algorithm of Aden-Antoniów et al. (2022), which utilizes the nearest-neighbor clustering algorithm of Zaliapin et al. (2008). This algorithm is robust for small samples and stable with M_c, yet sensitive to the d- and w-parameters that are defined by the user (we opted for 1.5 and 0.5 respectively, based on sensitivity tests). We post-processed the clusters to always keep the largest event in each one as the mainshock (instead of the earliest one).

3.2 Hypotheses testing for causal factors of induced seismicity

Following Grigoratos et al. (2020b) and Grigoratos et al. (2022), we hindcasted the observed seismicity with a set of competing statistical models to derive likelihood ratios that are then converted to p-values via reshuffling tests (McClure et al., 2017). First, injection and seismicity data are aggregated into spatial blocks of 5 to 10 km at fixed time intervals, on a monthly basis for SWD and on a daily basis for HF. Only blocks with nonzero volume for the corresponding operation and with at least 3 earthquakes above M_c are considered "active". Two block-specific hypotheses are constructed: (i) a null hypothesis model that assumes no relationship between injection and seismicity (total likelihood L_0), and (ii) an alternative model that does assume a relationship between injection and seismicity (total likelihood L_1). The ratio of L_1 to L_0 is defined as R. Although R values greater than 1.0 (i.e., $L_1 > L_0$) indicate that the alternative hypothesis is more likely than the null hypothesis, this criterion is not sufficient to statistically reject the null hypothesis. To do the latter, we need a reference statistical distribution for the ratio R in which the null hypothesis is true (R_{null}). This reference distribution enables the comparison of the two hypotheses in a rigorous way, even if they differ in model-complexity. R_{null} was empirically generated by reshuffling the injection data (with subsequent recalculation of L_1 and L_0; Grigoratos et al., 2022). R_{null} essentially reflects how likely it is for the earthquake recurrence model to find purely coincidental correlation between the observed seismicity and random injection data. By comparing the generated R_{null} values in each block with the single R value obtained from the real injection and seismicity time-series (R_{obs}), we can statistically determine how confident we are that the improved correlation of the alternative hypothesis is not coincidental. The metric used to quantify this confidence level is the statistical p-value, defined as $p = (\eta + 1)/(\kappa + 1)$, where η is the number of synthetic (reshuffled) datasets with R_{null} greater than the R_{obs} value from the real data, and κ is the total number of synthetic datasets (in our case 200). A p-value of 0.05, for example, translates to a confidence level C of 95% that the null hypothesis can be rejected (given that $C = 1 - p$).

The lower the p-value, the better the correlation between the seismicity and the oil and gas activity in question. Very low p-values, that is, below 0.05, signal that the examined human activity is a key triggering factor of the seismicity in that block (Grigoratos et al., 2022; McClure et al., 2017). P-values between 0.05 and 0.10 might flag blocks where a subset of the clusters is induced. Higher p-values above 0.20, and especially above 0.50, indicate that very little to no seismicity there was triggered by the analyzed type of human activity.

Here, we examined two external causal factors, namely HF and SWD. We ran the p-value analysis two times, assuming a single alternative causal factor at a time, each compared against the null hypothesis that assumes all earthquakes are of tectonic origin. Implementation details regarding the spatial oversampling used to account for epicentral location uncertainties are provided in Grigoratos et al. (2022) and Grigoratos and Wiemer (2023).

3.3 Generalized Seismogenic Index model with diffusion of disposal volumes

To hindcast the spatio-temporal changes in the seismicity rates we need a physics-based earthquake recurrence model that takes into account the external driving forces, i.e. the oil and gas activities. Since most of the stress changes are caused either directly or indirectly by the injected volumes, the model should use as input the injection rates of HF or SWD. We employed the framework of Grigoratos et al. (2020a, 2022), who expanded the Seismogenic Index model (Shapiro et al., 2010; Shapiro, 2015) to large-scale HF operations and wastewater disposal activities. They took into account the background tectonic rate and the stressing-rate dependency of the time lag between injection and seismicity rate changes (Norbeck and Rubinstein, 2018). The original Seismogenic Index model is itself a modified version of the Gutenberg-Richter relationship and predicts that the number of induced earthquakes is proportional to the pore pressure change, which can be approximated by the injected volume. It was first successfully used to hindcast induced seismicity related to hydraulic stimulations (Shapiro, 2015; Dinske and Shapiro, 2016; Kwiatek et al., 2024). The governing equations behind our earthquake recurrence model, as well as details on how the time-lags were modeled are available in Appendix A (Supplementary Material).

Following Grigoratos et al. (2020a), we acknowledge that SWD in one block will affect the pore pressure and stress field in a neighboring block. HF volumes, on the other hand, are injected into much less permeable formations and thus this effect is extremely localized relative to the size of our blocks. The latter is 5 km for HF and 10 km for SWD (Grigoratos et al., 2022). Thus, we distributed the SWD volumes of each well in space and time following the Theis (1935) equation for transient, radial flow in nonleaky vertically confined aquifers of infinite areal extent. The only parameter needed to compute the distribution factors is the large-scale diffusivity, D, which is meant to average out the diffusion process within both the disposal layer and the basement. We performed our computations for three different values of D equal to 0.3, 1.0 and 2.0 m^2/s and commented on the sensitivity of the results. More implementation details are provided in Grigoratos et al. (2020a) and in Appendix A (Supplementary Material).

3.4 Hydraulic Fracturing Radar

Following Grigoratos et al. (2022), we employed the Hydraulic Fracturing Radar (HFR) as an initial screening tool for HF within each region of interest. HFR gives a measure (per grid cell) of how many earthquakes happened close in space and time to HF operations, adjusted for how much HF activity actually took place there. This metric is employed only as a sanity check to confirm or question results stemming from the p-value analyses. To create HFR, first we plotted a 5 km base-grid with the percentage of earthquakes above M_c that occurred during or within 3 days of a HF stimulation and within 5 km from it (this percentage is called $EQ^{\%}_{HF}$). Next, $EQ^{\%}_{HF}$ is adjusted to account for the maximum total duration of stimulations within a block over the investigated study period. The reason for that adjustment is the observed asymmetry in the intensity of HF activities across blocks. HFR can be calculated using the declustered or non-declustered catalog. The distance threshold (5 km) is meant to cover the epicentral uncertainty of the earthquakes and the horizontal extension of the HF wells (toe-to-heel extension). The 3-day temporal buffer (after the stimulation end-date) is partly due to the uncertainty in the end-dates of the HF stimulations in the IHS database.

4 Results

4.1 HF

In this section we analyze the potential link between the observed seismicity in the FWB and HF. Figure 3b shows HFR values for the region, for the period between 2008 and September 2022, and for declustered earthquakes with magnitudes above 2. According to our own HFR-windows (section 3.4), just 4% of declustered earthquakes are associated with only 0.2% of the HF stimulations. The majority of blocks have low HFR values (below 0.10), validating the limited focus paid to HF in the literature. That said, there is one unnamed cluster at the border with Oklahoma that has very high HFR values and is very likely induced by HF. This is a novel finding, not previously reported in the literature. The other sequences do not appear linked to HF. The p-values tell the same story (Figure 3a), including the fact that the Lake Lewisville sequence does not appear affected by HF. Finally, the largest events linked to HF according to the HFR was M 3, and it occurred in July 17, 2011, less than 1 km away from the 2015 Venus M_w 4.0 event. The block hosting the M 3 event has however high p_{HF} value, indicating that the spatio-temporal link with HF might be coincidental.

4.2 SWD

The Ellenburger formation and the underlying basement are fractured (Ewing et al., 1990), enhancing permeability. This is why Zhai and Shirzaei (2018) assigned a diffusivity value of 0.7 m^2/s to the Ellenburger formation, which is the upper value from the range of Hornbach et al. (2015). Here, we show results for the declustered catalog and for the large-scale diffusivity D equal to 0.3 (Figure 4a), 1 (Figure S4) or 2 m^2/s (Figure 4b). The distributed SWD volumes, following pore pressure diffusion principles (equation S5), are shown in Figure S2b,c. After the diffusion process is applied, the SWD volumes have reached (to a varying degree) all the blocks of the basin (Figure S2b,c).

Even though the seismicity in the FWB appears spatially correlated with SWD operations, since the bulk of seismicity occurred within 15 km of high-rate SWD wells, most recorded earthquakes occurred in blocks with no SWD wells (Figure 2; S2a). The close proximity to causative SWD wells allows for potentially highly effective mitigation measures on a well-by-well basis. Even the very few far-field reported SWD clusters, did not exhibit an expanding seismicity front or cascading fault reactivation.

Overall, our results show that the spatial cells do not exhibit a persistent link with SWD activities. Figure 4 shows the statistical p-values for SWD (p_{SWD}) in the region, for the period between October 2008 and 2021 and for M ≥ 2. The results differ greatly with the adopted D value. For D = 2 m^2/s, SWD appears to be the sole causal factor behind the Irving-Dallas and Lake Lewisville sequences. These are novel findings, not previously reported in the literature. For lower D values however, the p_{SWD} values are above 0.05 (insignificant statistical confidence for association). Unfortunately, constraining this value based on hydrogeological factors is often a very subjective exercise (Grigoratos et al., 2020a, their table 1).

Curiously, no notable correlation (for any D value) is observed for the blocks that hosted the Venus, Azle–Reno or Cleburne earthquakes. The Airport sequence is linked to SWD for large D values, but not for D = 0.3 m^2/s, despite the very close proximity to wells. Perhaps a lower magnitude cut-off is needed for that sequence. Finally, the non-declustered catalog (Figure S5) leads to higher p-values than the declustered one, while adopting a higher M_c value (2.5) did not affect our findings.

We provide some caveats to the values reported and discussed above. Our framework assumes a consistent seismic response within each block across time, which does not appear to be the case in the FWB. Rather, the FWB is dominated by short-lived isolated sequences on a small subset of faults; the exception is the decadal-length Venus sequence, which is embedded within the highest SWD volumes in the basin (Quinones et al., 2019). Also, our analysis would have benefited from a more homogenous regional monitoring of the seismicity, since the completeness issues in the available earthquake catalogs are significant (see Data and code availability section). Therefore, although an elevated p-value implies that the grid cell overall is not reactive to the human activity in question, the possibility of individual (potentially notable) earthquakes within the block being induced still exists.

5 Conclusions

In this study, we apply for the first time an established probabilistic framework to examine the extent to which both SWD and HF have contributed to the unprecedented seismicity levels observed in the Fort Worth basin over the last 15 years. Our approach first hindcasts the seismicity rates after a given time on a spatial grid using either SWD or HF injection data as input, and then compares those rates against the null hypothesis of solely tectonic loading. In the end, each block is assigned a p-value, indicating the statistical confidence of the association with each oil and gas activity.

None of the main sequences (Venus, Azle–Reno, Airport, Irving-Dallas, Lake Lewisville, Cleburne) appear

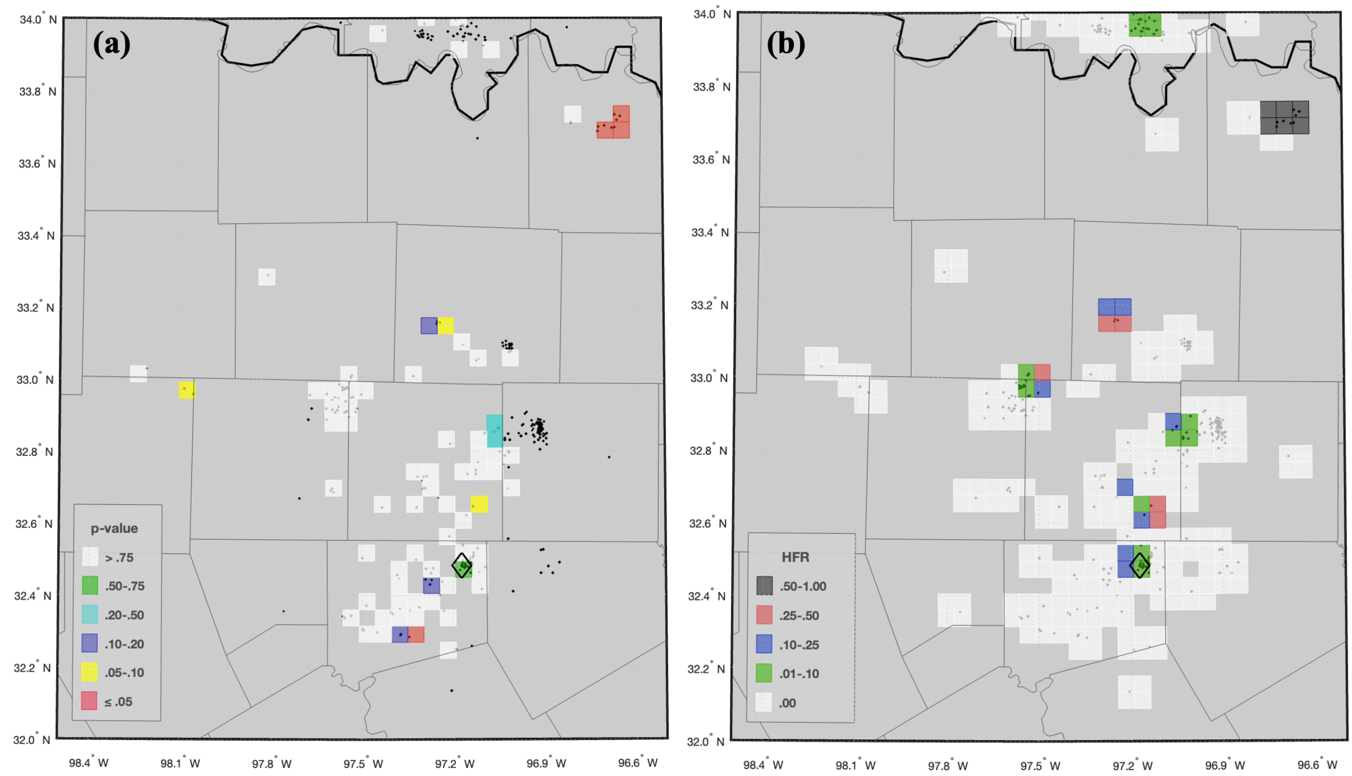

Figure 3 (a) Statistical p-values for HF between October 2008 and September 2022, with all declustered earthquakes above M 2 overlapped. Only "active" blocks are color-coded. (b) Mapped HFR values with all declustered earthquakes between 2008 and September 2022 above M 2 overlapped. The black diamond indicates the M_w 4.0 Venus earthquake. See Figure S3 for results using the non-declustered catalog.

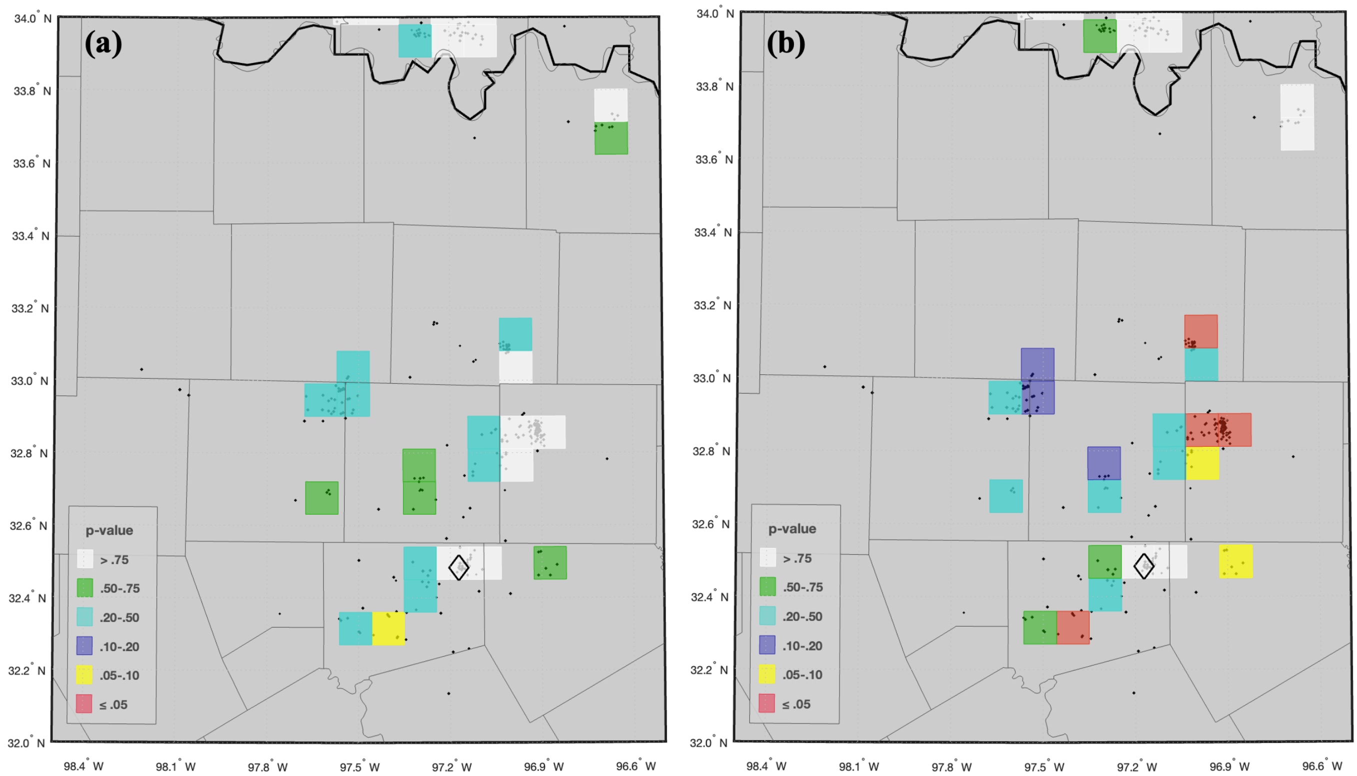

Figure 4 Statistical p-values for SWD between October 2008 and 2021, for D equal to 0.3 (a) and 2.0 (b) m^2/s, with all declustered earthquakes above M 2 overlapped. Only "active" blocks are color-coded. The black diamond indicates the M_w 4.0 Venus earthquake. State/county borders are also mapped. See Figure S4 for D equal to 1 m^2/s.

linked to HF operations. Within the investigated region, only one, so far undocumented, cluster at the border with Oklahoma is induced by HF.

At the basin-wide scale, seismicity in the FWB exhibits spatial correlation with SWD operations, with the bulk of seismicity occurring within 15 km of high-rate SWD wells. Our probabilistic findings regarding SWD are largely inconclusive since they are very sensitive to the chosen large-scale diffusivity value. For D = 2 m^2/s, SWD appears to have triggered the Irving-Dallas and Lake Lewisville sequences via far-field pore-pressure diffusion. This is a novel finding of our study that confirms hypotheses posited by Hornbach et al. (2015) and Gao et al. (2021). For lower D values however, confidence behind such an association is very low. Notably, no association is observed for the blocks that hosted the Venus (M_w 4.0), Azle–Reno or Cleburne earthquakes, contradicting previous research that linked these events with SWD using forward deterministic modeling. As discussed, our framework assumes a consistent seismic response within each block across time, which does not appear to be the case in the FWB, which may account for the discrepancy. Overall, we conclude that the FWB is not prone to widespread fault reactivation at the basin-wide scale, allowing for potentially highly effective mitigation measures on a well-by-well basis.

Acknowledgements

This material is based upon work supported by the U.S. Geological Survey under Grant No. G22AP00243 (FY2022) of the call G22AS00006. The Texas Seismological Network and Seismology Research (TexNet) and the State of Texas provided financial support under the University of Texas at Austin Award Number 201503664. We are grateful to Caroline Breton (BEG) for compiling the IHS Markit data and for assisting us in creating Figure 1. We thank Florent Aden-Antoniow for addressing inquiries related to his declustering code. The views and conclusions contained in this document are those of the authors and should not be interpreted as representing the opinions or policies of the U.S. Geological Survey. Mention of trade names or commercial products does not constitute their endorsement by the U.S. Geological Survey.

Data and code availability

Supplemental material regarding the input data and results is available as *csv* or *mat* files at https://zenodo.org/records/8327414 (add ".zip" extension to downloaded file). They include earthquake catalogs (declustered and non-declustered), gridded monthly SWD data, and resulting gridded p-values.

Sources of wastewater disposal data were the B3 database (https://www.b3insight.com/; last accessed December 11, 2022). Sources of HF data were the FracFocus Chemical Disclosure Registry (last accessed February 19, 2023) and the IHS Markit databases (last accessed March 29, 2023).

The following earthquake catalogs are available online: TexNet https://www.beg.utexas.edu/texnet-cisr/texnet/earthquake-catalog (last accessed October 22, 2024), ANSS ComCat https://earthquake.usgs.gov/earthquakes/search/ (last accessed February 20, 2023). The code used for the declustering is based on scripts that can be found at https://zenodo.org/record/5838353. The python code for the duplicate-removal process can be found at https://github.com/klunk386/CatalogueTool-Lite/tree/master/OQCatk. All the figures were made using the Matlab software package (http://www.mathworks.com, last accessed March 2023). The analyses presented in this paper greatly benefited from the high-performance computing resources available at SED.

Competing interests

The authors declare no competing interests.

References

Aden-Antoniów, F., Frank, W. B., and Seydoux, L. An Adaptable Random Forest Model for the Declustering of Earthquake Catalogs. *Journal of Geophysical Research: Solid Earth*, 127(2), Feb. 2022. doi: 10.1029/2021jb023254.

DeShon, H. R., Hayward, C. T., Ogwari, P. O., Quinones, L., Sufri, O., Stump, B., and Magnani, M. B. Summary of the North Texas Earthquake Study Seismic Networks, 2013–2018. *Seismological Research Letters*, 90(1):387–394, Nov. 2019. doi: 10.1785/0220180269.

Dinske, C. and Shapiro, S. Performance test of the Seismogenic index model for forecasting magnitude distributions of fluid-injection-induced seismicity. In *SEG Technical Program Expanded Abstracts 2016*. Society of Exploration Geophysicists, 2016. doi: 10.1190/segam2016-13958126.1.

Ewing, T., Budnik, R., Ames, J., Ridner, D., and Dillon, R. *Tectonic Map of Texas, scale 1: 750,000*. University of Texas Bureau of Economic Geology, Austin, Texas, 1990.

Frohlich, C. Two-year survey comparing earthquake activity and injection-well locations in the Barnett Shale, Texas. *Proceedings of the National Academy of Sciences*, 109(35):13934–13938, Aug. 2012. doi: 10.1073/pnas.1207728109.

Frohlich, C., Potter, E., Hayward, C., and Stump, B. Dallas-Fort Worth earthquakes coincident with activity associated with natural gas production. *The Leading Edge*, 29(3):270–275, Mar. 2010. doi: 10.1190/1.3353720.

Frohlich, C., Hayward, C., Stump, B., and Potter, E. The Dallas-Fort Worth Earthquake Sequence: October 2008 through May 2009. *Bulletin of the Seismological Society of America*, 101(1):327–340, Jan. 2011. doi: 10.1785/0120100131.

Frohlich, C., DeShon, H., Stump, B., Hayward, C., Hornbach, M., and Walter, J. I. A historical review of induced earthquakes in Texas. *Seismological Research Letters*, 87(4):1022–1038, May 2016. doi: 10.1785/0220160016.

Gao, S., Nicot, J.-P., Hennings, P. H., La Pointe, P., Smye, K. M., Horne, E. A., and Dommisse, R. Low pressure buildup with large disposal volumes of oil field water: A flow model of the Ellenburger Group, Fort Worth Basin, northcentral Texas. *AAPG Bulletin*, 105(12):2575–2593, Dec. 2021. doi: 10.1306/03252120159.

Grigoratos, I. and Wiemer, S. Probabilistic identification of seismicity triggered by oil and gas activities and its effects on seismic hazard. Final Technical Report for the USGS Earthquake Hazards Program Grant G22AP00243, USGS, 2023.

Grigoratos, I., Rathje, E., Bazzurro, P., and Savvaidis, A. Earthquakes Induced by Wastewater Injection, Part I: Model Development and Hindcasting. *Bulletin of the Seismologi-*

cal Society of America, 110(5):2466–2482, Aug. 2020a. doi: 10.1785/0120200078.

Grigoratos, I., Rathje, E., Bazzurro, P., and Savvaidis, A. Earthquakes Induced by Wastewater Injection, Part II: Statistical Evaluation of Causal Factors and Seismicity Rate Forecasting. *Bulletin of the Seismological Society of America*, 110(5):2483–2497, Aug. 2020b. doi: 10.1785/0120200079.

Grigoratos, I., Savvaidis, A., and Rathje, E. Distinguishing the Causal Factors of Induced Seismicity in the Delaware Basin: Hydraulic Fracturing or Wastewater Disposal? *Seismological Research Letters*, 93(5), 2022. doi: 10.1785/0220210320.

Grigoratos, I., Poggi, V., Danciu, L., and Monteiro, R. Homogenizing instrumental earthquake catalogs – a case study around the Dead Sea Transform Fault Zone. *Seismica*, 2(2), Nov. 2023. doi: 10.26443/seismica.v2i2.402.

Grigoratos, I., Savvaidis, A., and Wiemer, S. Revisiting the Seismicity in the Eagle Ford Shale: The Overlooked Role of Wastewater Disposal. *The Seismic Record*, 5(2):145–154, Apr. 2025a. doi: 10.1785/0320250010.

Grigoratos, I., Savvaidis, A., and Wiemer, S. Seven Thousand Felt Earthquakes in Oklahoma and Kansas Can Be Confidently Traced Back to Oil and Gas Activities. *GeoHazards*, 6(3), 2025b. doi: 10.3390/geohazards6030036.

Hennings, P. H., Nicot, J., Gao, R. S., DeShon, H. R., Lund Snee, J., Morris, A. P., Brudzinski, M. R., Horne, E. A., and Breton, C. Pore Pressure Threshold and Fault Slip Potential for Induced Earthquakes in the Dallas-Fort Worth Area of North Central Texas. *Geophysical Research Letters*, 48(15), Aug. 2021. doi: 10.1029/2021gl093564.

Hornbach, M. J., DeShon, H. R., Ellsworth, W. L., Stump, B. W., Hayward, C., Frohlich, C., Oldham, H. R., Olson, J. E., Magnani, M. B., Brokaw, C., and Luetgert, J. H. Causal factors for seismicity near Azle, Texas. *Nature Communications*, 6(1), Apr. 2015. doi: 10.1038/ncomms7728.

Hornbach, M. J., Jones, M., Scales, M., DeShon, H. R., Magnani, M. B., Frohlich, C., Stump, B., Hayward, C., and Layton, M. Ellenburger wastewater injection and seismicity in North Texas. *Physics of the Earth and Planetary Interiors*, 261:54–68, Dec. 2016. doi: 10.1016/j.pepi.2016.06.012.

Justinic, A. H., Stump, B., Hayward, C., and Frohlich, C. Analysis of the Cleburne, Texas, Earthquake Sequence from June 2009 to June 2010. *Bulletin of the Seismological Society of America*, 103 (6):3083–3093, Oct. 2013. doi: 10.1785/0120120336.

Kwiatek, G., Grigoratos, I., and Wiemer, S. Variability of Seismicity Rates and Maximum Magnitude for Adjacent Hydraulic Stimulations. *Seismological Research Letters*, 96(2A), 2024. doi: 10.1785/0220240043.

Magnani, M. B., Blanpied, M. L., DeShon, H. R., and Hornbach, M. J. Discriminating between natural versus induced seismicity from long-term deformation history of intraplate faults. *Science Advances*, 3(11), Nov. 2017. doi: 10.1126/sciadv.1701593.

McClure, M., Gibson, R., Chiu, K., and Ranganath, R. Identifying potentially induced seismicity and assessing statistical significance in Oklahoma and California. *Journal of Geophysical Research: Solid Earth*, 122(3):2153–2172, Mar. 2017. doi: 10.1002/2016jb013711.

Norbeck, J. H. and Rubinstein, J. L. Hydromechanical Earthquake Nucleation Model Forecasts Onset, Peak, and Falling Rates of Induced Seismicity in Oklahoma and Kansas. *Geophysical Research Letters*, 45(7):2963–2975, Apr. 2018. doi: 10.1002/2017gl076562.

Ogwari, P. O., DeShon, H. R., and Hornbach, M. J. The Dallas-Fort Worth Airport Earthquake Sequence: Seismicity Beyond Injection Period. *Journal of Geophysical Research: Solid Earth*, 123 (1):553–563, Jan. 2018. doi: 10.1002/2017jb015003.

Quinones, L. *Tracking Induced Seismicity in the Fort Worth Basin, Texas and Northern Oklahoma Using Local and Large-N Style Arrays*. PhD thesis, Southern Methodist University, 2021.

Quinones, L., DeShon, H. R., Jeong, S., Ogwari, P., Sufri, O., Holt, M. M., and Kwong, K. B. Tracking Induced Seismicity in the Fort Worth Basin: A Summary of the 2008–2018 North Texas Earthquake Study Catalog. *Bulletin of the Seismological Society of America*, 109(4), 2019. doi: 10.1785/0120190057.

Savvaidis, A., Young, B., Huang, G. D., and Lomax, A. TexNet: A Statewide Seismological Network in Texas. *Seismological Research Letters*, 2019. doi: 10.1785/0220180350.

Scales, M. M., DeShon, H. R., Magnani, M. B., Walter, J. I., Quinones, L., Pratt, T. L., and Hornbach, M. J. A Decade of Induced Slip on the Causative Fault of the 2015 Mw 4.0 Venus Earthquake, Northeast Johnson County, Texas: Induced Seismicity in Johnson County, TX. *Journal of Geophysical Research: Solid Earth*, 122(10):7879–7894, Oct. 2017. doi: 10.1002/2017jb014460.

Segall, P. and Lu, S. Injection-induced seismicity: Poroelastic and earthquake nucleation effects. *Journal of Geophysical Research: Solid Earth*, 120(7), 2015. doi: 10.1002/2015jb012060.

Shapiro, S. A. *Fluid-Induced Seismicity*. Cambridge University Press, Apr. 2015. doi: 10.1017/cbo9781139051132.

Shapiro, S. A., Dinske, C., Langenbruch, C., and Wenzel, F. Seismogenic index and magnitude probability of earthquakes induced during reservoir fluid stimulations. *The Leading Edge*, 29(3): 304–309, Mar. 2010. doi: 10.1190/1.3353727.

Theis, C. V. The relation between the lowering of the Piezometric surface and the rate and duration of discharge of a well using ground-water storage. *Eos, Transactions American Geophysical Union*, 16(2):519–524, 1935. doi: 10.1029/TR016i002p00519.

Walsh, F. R. and Zoback, M. D. Probabilistic assessment of potential fault slip related to injection-induced earthquakes: Application to north-central Oklahoma, USA. *Geology*, 44(12):991–994, Dec. 2016. doi: 10.1130/g38275.1.

Zaliapin, I., Gabrielov, A., Keilis-Borok, V., and Wong, H. Clustering Analysis of Seismicity and Aftershock Identification. *Physical Review Letters*, 101(1), 2008. doi: 10.1103/physrevlett.101.018501.

Zhai, G. and Shirzaei, M. Fluid Injection and Time-Dependent Seismic Hazard in the Barnett Shale, Texas. *Geophysical Research Letters*, 45(10):4743–4753, May 2018. doi: 10.1029/2018gl077696.